Developmental Biology 359 (2011) 277–288

Contents lists available at SciVerse ScienceDirect

Developmental Biology

journal homepage: www.elsevier.com/developmentalbiology

# An AT-hook gene is required for palea formation and floral organ number control in rice

Yun Jin [a,1], Qiong Luo [b,1], Hongning Tong [a,1], Aiju Wang [c], Zhijun Cheng [d], Jinfu Tang [a], Dayong Li [a], Xianfeng Zhao [a], Xiaobing Li [a], Jianmin Wan [d], Yuling Jiao [a], Chengcai Chu [a], Lihuang Zhu [a,*]

[a] State Key Laboratory of Plant Genomics and National Center for Plant Gene Research (Beijing), Institute of Genetics and Developmental Biology, Chinese Academy of Sciences, Beijing 100101, China
[b] Ministry of Education Key Laboratory of Agriculture Biodiversity for Plant Disease Management, Key Laboratory of Plant Pathology of Yunnan Province, Yunnan Agricultural University, Kunming 650201, China
[c] Key Laboratory of Genome Science and Information, Beijing Institute of Genomics, Chinese Academy of Sciences, Beijing 100029, China
[d] National Key Facility for Crop Gene Resources and Genetic Improvement, Institute of Crop Science, Chinese Academy of Agricultural Sciences, Beijing 100081, China

ARTICLE INFO

*Article history:*
Received for publication 28 April 2011
Revised 29 August 2011
Accepted 30 August 2011
Available online 7 September 2011

*Keywords:*
Rice
Flower
Palea
Meristem

ABSTRACT

Grasses have highly specialized flowers and their outer floral organ identity remains unclear. In this study, we identified and characterized rice mutants that specifically disrupted the development of palea, one of the outer whorl floral organs. The *depressed palea1* (*dp1*) mutants show a primary defect in the main structure of palea, implying that palea is a fusion between the main structure and marginal tissues on both sides. The sterile lemma at the palea side is occasionally elongated in *dp1* mutants. In addition, we found a floral organ number increase in *dp1* mutants at low penetration. Both the sterile lemma elongation and the floral organ number increase phenotype are enhanced by the mutation of an independent gene *SMALL DEGENERATIVE PALEA1* (*SDP1*), whose single mutation causes reduced palea size. E function and presumable A function floral homeotic genes were found suppressed in the *dp1–2* mutant. We identified the *DP1* gene by map-based cloning and found it encodes a nuclear-localized AT-hook DNA binding protein, suggesting a grass-specific role of chromatin architecture modification in flower development. The *DP1* enhancer *SDP1* was also positional cloned, and was found identical to the recently reported *RETARDED PALEA1* (*REP1*) gene encoding a TCP family transcription factor. We further found that *SDP1*/*REP1* is downstreamly regulated by *DP1*.



## Introduction

Based on the studies of homeotic mutants in several eudicot species, especially the model plant species *Arabidopsis thaliana* and *Antirrhinum majus*, the ABC model was proposed to elucidate flower organ formation (Bowman et al., 1991; Coen and Meyerowitz, 1991). In this model, three classes of genes, A, B and C, work in a combinatorial fashion to confer organ identities of four whorls (Krizek and Fletcher, 2005). Class A genes affect sepals and petals, class B genes affect petals and stamens, and class C genes affect stamens and carpels. Another class of genes (sometimes termed E function) genes, which are meristem identity genes required to specify all four whorls, extends the model (reviewed in Krizek and Fletcher, 2005). Further studies in other plant species have demonstrated that the ABC model in general is applicable to eudicots and monocots (Ambrose et al., 2000; Dreni et al., 2007; Nagasawa et al., 2003; Yamaguchi and Hirano, 2006).

Monocots differ considerably from dicots in floral organ morphology, especially for non-reproductive floral organs (Bommert et al., 2005; Kellogg, 2001; Zanis, 2007). Poaceae, the grass family, as one of the largest monocot families, have highly specialized flowers, whose structural units are spikelets and florets. In rice, a spikelet is composed of two rudimentary glumes, two sterile lemmas (also named empty glumes), and a floret which consists of one lemma, one palea and two lodicules at the outer whorls, and six stamens and one carpel at the inner whorls (Bommert et al., 2005; Kater et al., 2006; Kellogg, 2001; Kyozuka et al., 2000). Although the two lodicules have been proved to be homologous to petals (Ambrose et al., 2000; Kang et al., 1998; Nagasawa et al., 2003; Whipple et al., 2007; Xiao et al., 2003), views on the specification and the equivalence of palea and lemma remain controversial due to their confusing morphological characters. Initially, palea has been considered as prophyll-like structure and lemma as a bract-like structure (Bell and Bryan, 1991; Bell and Bryan, 2008; Clifford, 1987; Kellogg, 2001; Zanis, 2007). Other researchers have suggested that palea and lemma together are the equivalents of the eudicot sepal (Ambrose et al., 2000; Kyozuka et al., 2000; Shinozuka et al., 1999). The third view prefers that only the palea is equivalent to the sepal of eudicot (Luo et al., 2005; Schmidt and Ambrose, 1998).

* Corresponding author.
*E-mail address:* lhzhu@genetics.ac.cn (L. Zhu).
[1] These authors contributed equally to this work.

0012-1606/$ – see front matter © 2011 Elsevier Inc. All rights reserved.
doi:10.1016/j.ydbio.2011.08.023

Consistent with this controversy of sepal equivalent organ in rice and other grasses, class A genes in rice remain difficult to determine. Similar to rice, the maize outer whorl organ identity remains elusive that molecular dissection of regulatory pathways has just started (Thompson et al., 2009; Whipple et al., 2010).

In order to understand the molecular regulation of rice outer floral whorl development, we identified and characterized more palea defective mutants. We isolated a new allele of our previously reported *palealess1* (*pal1*) mutant (Luo et al., 2005). We further found that the classical rice mutant *depressed palea1* (*dp1*) is allelic to the *pal1* mutants, and the name *dp1* is used thereafter. We identified another palea deficient mutant *small degenerative palea1* (*sdp1*). In addition to palea defects, we found that *DP1* affects sterile lemma identity and floral meristem activity. Both functions were enhanced by *SDP1*. We identified *DP1* and *SDP1* by positional cloning and demonstrated that *DP1* encodes an AT-hook protein with DNA binding activity and possible chromatin state regulation ability. The *Arabidopsis* genes most closely related to *DP1* did not affect flower development (Xiao et al., 2009). This may be attributed to potential functional divergence or gene duplication and function redundancy during evolution. We further revealed that *DP1* regulates floral organ identity and meristem activity through mediating expression of floral E function genes *OsMADS1*, *OsMADS6* and *OsMADS17*, and AP1-like gene *OsMADS15*. Thus, *DP1* appears to be a novel regulator of rice flower development, possibly via chromatin architecture control.

## Materials and methods

### *Plant materials*

Four rice mutants, *dp1–1*, *dp1–2*/*pal1*, *dp1–3* and *sdp1*/*rep1–3* were used in this study. The recessive mutant *dp1–1*, previously named *dp1* (Iwata et al., 1984; Yoshimura et al., 1997), was in the *japonica* background, and was requested from the SHIGEN Oryzabase (http://www.shigen.nig.ac.jp). The *dp1–2* allele, previously reported as *pal1*, was a spontaneous mutation in the *indica* subspecies SARIII-93-369 background (Luo et al., 2005). An addition allele *dp1–3* was obtained from anther culture of autotetrapolyploid rice (Qin et al., 2005). The *sdp1*/*rep1–3* mutant was obtained in plants derived from tissue culture in the *japonica* subspecies Nipponbare. Corresponding cultivars were used as wild-type strains for phenotype comparison. The rice strain Taipei 309 was used for transformation unless otherwise specified. For all the observations in this study, plants were grown from May to October in the farm field of the Institute of Genetics and Developmental Biology, Chinese Academy of Sciences in Beijing. Morphology observations were carried under a stereomicroscope (SZX16, Olympus, Tokyo).

### *Scanning electron microscopy (SEM) observation*

Samples were fixed in 2.5% glutaraldehyde solution. Fixed samples were dehydrated with gradual ethanol series, dried by critical-point drying method using liquid carbon dioxide (Model HCP-2, Hitachi, Tokyo), gold-coated with an Edwards E-1010 ion sputter coater (Hitachi, Tokyo), and then observed using a S-3000N variable pressure scanning electron microscope (Hitachi, Tokyo).

### *Positional cloning*

The *dp1* locus was mapped by using an $F_2$ population of *dp1–2* and Sheng47 (spp. *indica*). The locus was mapped to a region between cleaved-amplified polymorphic sequence (CAPS) markers M4 and M6 on the short arm of chromosome 6 (Luo et al., 2005). We further developed two new CAPS markers M9 and dM1 in this region (Table S2) to narrow the locus to a 10 kb region between M4 and dM1 (Fig. 6A).

The *sdp1* locus was mapped by using an $F_2$ population of *sdp1* and Minghui 63 (spp. *indica*). The locus was mapped to a 92 kb region between two sequence-tagged site markers, S14533 and S14625 (Fig. S6).

### *Vector construction and plant transformation*

Primer sequences used for vector construction are listed in Table S2 in the Supplementary data. For complementation of the *dp1–2* mutant, a 9292 bp genomic fragment containing the entire *DP1* coding sequence, 5728 bp of the 5′ upstream region and 2577 bp of the 3′ downstream region was digested form PAC clone P0548D03, and cloned into the pCAMBIA1300 vector to generate plasmid p1300-DP1. For RNA interference analysis, a fragment of the *DP1* cDNA (864 bp–1276 bp of the coding region) was amplified and cloned into pUCCRNAi vector by forward and reverse insertions. The entire fragment was subcloned into pCAMBIA1300A under the rice *ACTIN1* promoter. For pDP1::*GUS* and pDP1::*DP1-GFP* (green fluorescent protein), specific primers with suitable adaptors were designed to amplify relative sequences (Table S2), and cloned into pCAMBIA1301 or CAMV35S-sGFP(S65T)-Nos (Niwa et al., 1999), respectively. These vectors were subsequently transformed into calli derived from mature rice seeds through *Agrobacterium*-mediated methods (Hiei et al., 1994).

### *RT-PCR and quantitative real time PCR (qRT-PCR)*

Total RNA was extracted using TRIZOL (Invitrogen, Carlsbad). The RNA was pre-treated with RNase-free DNase I (Takara, Shiga), and first-strand cDNA was synthesized from 2 μg of total RNA using reverse transcriptase (M-MLV, Promega, Madison). The reverse transcription product was used for PCR with gene specific primers (Table S2). Rice *ACTIN1* was used as the internal reference. For qRT-PCR, SYBR Green I was added to the reaction system and run on a Chromo 4 real-time PCR detection system (Bio-Rad, Hercules) according to the manufacturer's instructions. Three replicates were carried out for each gene, and each analysis was biologically repeated at least twice. Student's *t*-test was used to determine significant changes ($P<0.05$).

### *GUS Staining and GFP observation*

GUS staining was performed as previously described (Jefferson, 1989). The construct DP1-GFP was used to transform rice plant or to infiltrate tobacco leaf epidermic cells by *Agrobacterium*-mediated methods (Sparkes et al., 2006). Tobacco leaf tissue with GFP fluorescence was directly immersed in DAPI (4,6-diamidino-2-phenylindole) solution (1 μg/ml) for nuclear staining. GFP and DAPI fluorescence was observed under a confocal fluorescence microscope (Olympus FV500).

### *Electrophoretic mobility shift assay*

The assay was performed as described previously (Yin et al., 2005). Briefly, *DP1* coding region was amplified (Table S2) and cloned into pETMALc-H (Pryor and Leiting, 1997). The recombinant DP1-MBP (Maltose binding protein) was purified from *Escherichia coli* using HIS-Ni resin (GE Health, Piscataway). A random AT-rich oligo was synthesized, annealed and labeled with [gamma-$^{32}$P]-ATP and about 0.5 ng of probes was used for each binding assay (Matsushita et al., 2007; Nieto-Sotelo et al., 1994). For competition experiment, excessive unlabeled probes were added to the reactions with 50-fold molar ratios compared to labeled probe.

### *RNA in situ hybridization*

A gene-specific region of *DP1* (645 bp–954 bp of the coding region) (Table S2) and labeled using a DIG RNA labeling kit (Roche, Mannheim). Samples were fixed in FAA (10% formaldehyde, 5% acetic acid, 47.5% ethanol), dehydrated and embedded in Paraplast Plus (Sigma-Aldrich,

St. Luis). Tissues were sliced into 8 μm sections using a microtome (RM2135, Leica, Wetzlar) and affixed to Poly-Prep slides (Sigma-Aldrich, St. Luis). Pretreatment of sections, hybridization and immunological detection was performed as described (Li et al., 2005).

## Results

### *DP1 and SDP1 affect palea formation*

In wild type rice flowers, the inner whorls, including a pistil, six stamens, and two lodicules, are subtended by a palea and a lemma to form a floret (Figs. 1A, B). A floret together with a pair of sterile lemmas and a pair of rudimentary glumes, which subtend at the floret base, constitute a spikelet.

To reveal the molecular mechanism regulating rice palea and lemma development, we identified mutants with defect in palea morphology. We obtained an additional allele *dp1–3* from anther culture of autotetrapolyploid rice for the previously reported recessive *dp1–2/pal1* mutant (Luo et al., 2005). An allelism test revealed that both mutants were allelic to the classical mutant *dp1–1* (previously described as *dp1*). An independent recessive *sdp1* mutant was obtained in plants derived from tissue culture.

Compared to wild type plants, *dp1–2* showed normal vegetative development and flowering time, as well as normal inflorescence morphology. Flowers of *dp1–2* displayed clear defects when compared to wild type (Figs. 1A–D). In *dp1–2* spikelets, the paleas degenerated to two leaf-like organs residing beside the lodicules, but retain normal lemmas and other floral organs, forming an open structure with partially exposed inner organs (Figs. 1C–E, M). Spikelets of *dp1–3* showed a similar phenotype as *dp1–2*, whereas spikelets of *dp1–1* exhibited an obviously milder phenotype with most of flowers showing smaller than normal paleas without extra leaf-like organs (Table 1).

To study the identity of the abnormal leaf-like organ pairs observed in *dp1–2* and *dp1–3*, we examined morphological differences in the palea and lemma epidermal cells in these mutants and in the wild type by SEM. In a wide type rice plant, the palea had distinctive marginal tissue, which is absent in the lemma (Prasad and Vijayraghavan, 2003; Prasad et al., 2005; Yadav et al., 2007). This marginal region of palea lacks epicuticular or silicified thickening, and differs from the rest of palea with a unique smooth epidermis (Figs. 2A, B). By contrast, the central region of palea shares similar cellular morphology with lemma that both of them comprise regular epidermal bulges formed by cuticular thickening (Fig. 2A). In *dp1–2* flowers, the extra leaf-like organ pairs beside lodicules showed a smooth epidermal surface similar

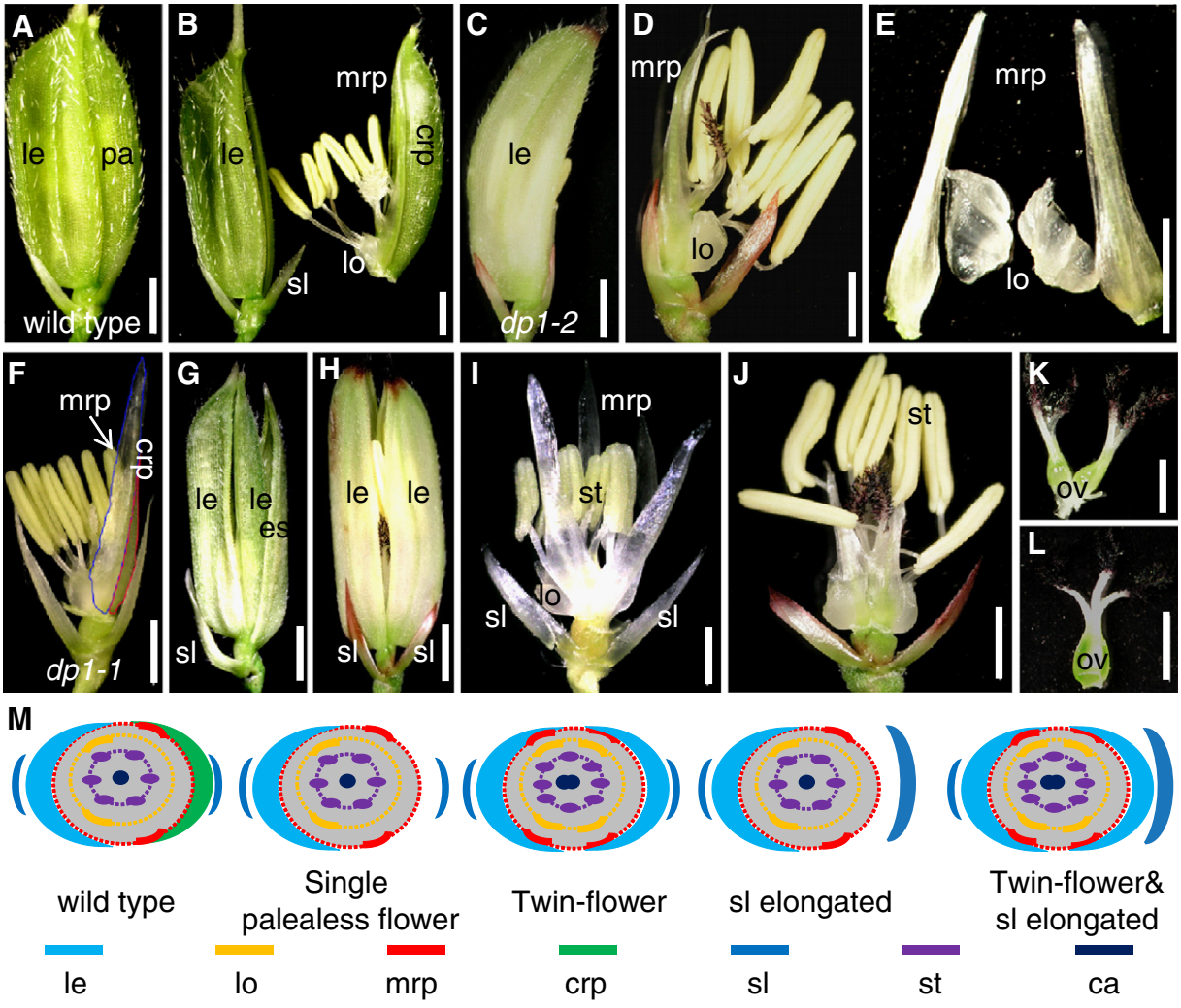


**Fig. 1.** Phenotype of *dp1* mutants. (A, B) Normal spikelets of a wild type. (B) Lemma and palea were separated to show inner organs. (C–E) Spikelets of *dp1–2*. (D) Lemma was removed to show inner organs. The presumed mrp was indicated. (E) The detached mrp and lodicules were shown. (F) A spikelet of *dp1–1* with lemma removed. Mrp and crp were indicated by blue and red circle respectively. (G) A spikelet with elongated sterile lemma. (H–L) Phenotypes of twin-flower spikelets of *dp1–2*. (I) Four presumed mrps were presented in a twin-flower. (J) Seven stamens were indicated. (K, L) Carpels consisted of two ovaries with four stigmas (K) or one ovary with three stigmas (L). (M) A schematic diagram of spikelet phenotypes of wild type and *dp1–2* mutant. Mrp and crp are separated as independent organs in the diagram. le, lemma; pa, palea; lo, lodicule; sl, sterile lemma; st, stamen; ov, ovule; ca, carpel; esl, elongated sterile lemma; mrp, marginal region of palea; crp, central region of palea. Scale bars = 1 mm.

**Table 1**
Proportions of the major flower phenotypes in mutants and transgenic plants.

| | dp1−2 | dp1−3 | dp1−1 | sdp1/rep1−3 | dp1−2 sdp1/rep1−3 | DP1i−1 | DP1i−2 |
|---|---|---|---|---|---|---|---|
| Observation no. | 183 | 136 | 158 | 840 | 115 | 137 | 138 |
| Palealess | 183 (100%) | 136 (100%) | 0 | 0 | 115 (100%) | 0 | 124 (89.9%) |
| Small palea | 0 | 0 | 158 (100%) | 837 (99.6%) | 0 | 89 (65.0%) | 14 (10.1%) |
| Twin-flower | 9 (4.9%) | 9 (6.6%) | 5 (3.2%) | 3 (0.36%) | 74 (64.3%) | 22 (16.1%) | 66 (47.8%) |
| Sterile lemma elongation | 7 (3.8%) | 11 (8.1%) | 3 (1.9%) | 0 | 98 (85.2%) | 2 (1.5%) | 3 (2.2%) |

to that of the wild type marginal region of palea (Figs. 2B–D). Together with the shared position, the cellular morphology observations suggest these leaf-like organ pairs are likely retained marginal regions of palea. This notion is further supported by observations from *dp1–1*, the weaker allele. In *dp1–1* flowers, while paleas were repressed to a smaller size (Fig. 1F), the marginal region of palea appeared to be unaffected, which remained attached to the central region of palea. Instead, the severely affected central region of palea accounted for the reduction of palea size (Fig. 1F). Taken together, only the central region of palea development, but not the marginal region of palea development, was affected by the *dp1* mutation (Fig. 1M).

To further characterize the developmental defects of paleas in *dp1* mutants, we examined early stages of spikelet development by SEM. In a wild type rice, the palea primordium is visible at stage Sp 4 between the formation of the lemma primordium (Sp 3) and the formation of lodicule and stamen primordia (Sp 5–6; Figs. 3A–C) (Ikeda et al., 2004). In *dp1–2*, the formation of the palea primordium appeared to be slightly delayed at stage Sp 4 (Fig. 3D). After that, the development course of palea primordium continued to be retarded or arrested (Fig. 3E), leading to a palea rudiment covered by the expended sterile lemma after stage Sp 7 (Fig. 3F).

Effects of *sdp1* mutation were similarly restricted to the palea development, with most flowers (>99%) showing small degenerative paleas but normal lodicules and inner organs (Figs. 4A–C; Table 1).

### *DP1 and SDP1 affect sterile lemma identity on the palea side*

In addition to palea development, we found that the sterile lemma identity was affected by the *dp1* mutation, albeit at a much lower frequency. In a wild type rice spikelet, one fertile floret is subtended by a pair of sterile lemmas (Figs. 1A, B), which have smooth epidermal cells with no cuticular thickenings (Prasad et al., 2005). In contrast, we observed elongation of the sterile lemma on the palea side in all three *dp1* mutants at a frequency of 2–8% (Figs. 1G, M; Table 1). The elongated sterile lemmas showed obvious epicuticular thickening without a

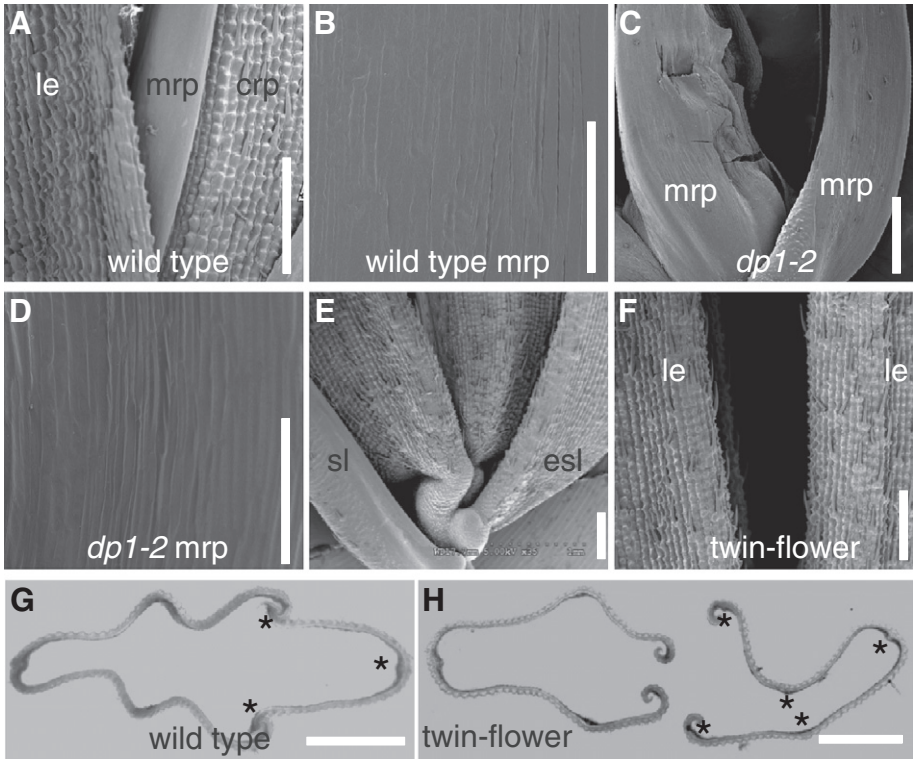


**Fig. 2.** Characterization of the spikelet outer organs. (A) SEM observation of lemma and palea epidermis structure of a wild type spikelet. (B) Magnified wild type palea margin. (C, D) SEM observation shows the leaf-like organs (presumed marginal region of palea) have smooth epidermis (C), as magnified in (D). (E, F) SEM observation of a *dp1–2* spikelet with elongated sterile lemma (E) and twin-flower (F). (G, H) Cross sections of lemma and palea of wild type spikelet (G) and twin-flower spikelet (H). Vascular bundles at the palea side were indicated by asterisks. le, lemma; mrp, marginal region of palea; crp, central region of palea; sl, sterile lemma; esl, elongated sterile lemma. Scale bars = 500 μm in (A), (E) and (F); = 100 μm in (B–D); = 1 mm in (G) and (H).

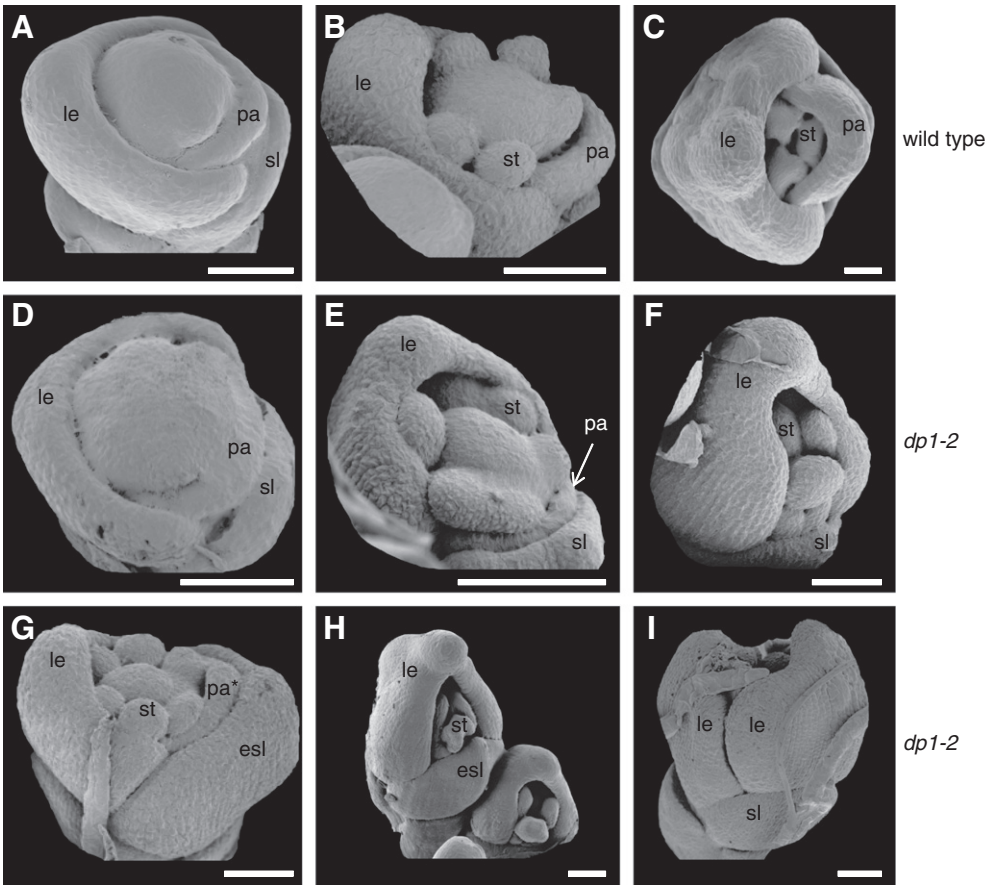


**Fig. 3.** SEM observation of the spikelet organ developmental process of wild type and *dp1–2*. (A) Palea primordium initiates in wild type (Sp4). (B) Palea primordium grows up when stamen initiates in wild type (Sp5–6). (C) Palea and lemma form a near-close structure when stamen differentiates in wild type (Sp7). (D) Palea primordium initiates in *dp1–2*. (E) Palea primodium growth was arrested in *dp1–2* at Sp5–6, while other organs develop normally. (F) Palea was covered by sterile lemma. (G) Elongated sterile lemma at Sp56. The palea (indicated by pa*) is presumed to develop to a lemma in twin-flower. (H) Elongated sterile lemma at Sp7. (I) Twin-flower. le, lemma; pa, palea; sl, sterile lemma; st, stamen; esl, elongated sterile lemma. Scale bars = 50 μm.

smooth marginal region, suggesting that they might have acquired the lemma identity (Fig. 2E).

We found that the overgrowth of sterile lemmas occurred earlier during spikelet development. In some *dp1-2* spikelets, sterile lemmas at the palea side exhibited a similar height as lemmas as early as stage Sp 6 (Fig. 3G). The growth rate of such elongated sterile lemmas was comparable to the wild type paleas and lemmas (Figs. 3G, H).

The sterile lemma elongation phenotype was enhanced by the *sdp1* mutation. Although no elongated sterile lemma was observed in *sdp1* flowers as in any wild type ones (N>800, Table 1), most *dp1–2 sdp1* double mutant flowers (>85%) contained elongated sterile lemmas (Figs. 4D, E). Still, such elongated sterile lemmas were only found on the adaxial side, where a palea would form in wild type spikelets.

### *DP1 and SDP1 affect floral organ number*

In addition to affecting palea and sterile lemma development, both *DP1* and *SDP1* genes regulate floral organ number at a low penetrance. In *dp1–2*, ~5% spikelets, which we named "twin-flowers", exhibited a nearly closed structure with an additional lemma-like organ in place of paleas (Figs. 1G, H, M). This lemma-like organ shared the same vascular number as that of a lemma, but different from a typical palea (Figs. 2G, H). Such lemma-like organ does not contain the palea-specific marginal region either (Fig. 2F). The presumably retained palea margin pairs were also doubled in such twin-flowers (Fig. 1I). In the inner whorls, the floral organ numbers were often near-doubled in twin-flowers, including four lodicules, seven or eight stamens and two ovaries with four stigmas or one ovary with three stigmas (Figs. 1J–M). The formation of two lemmas in such twin-flowers initiated early during spikelet development as demonstrated by SEM observation (Fig. 3I). Such twin-flower spikelets would lead to the formation of two separate seeds or one conjoined seed containing two embryos (Fig. S1). We found that the floral meristems of twin-flowers were enlarged when compared to a wild type floral meristem (Fig. S2). Similar twin-flower phenotype was identified in other *dp1* alleles and in *sdp1* at low penetrance (Fig. 4K; Table 1).

Strikingly, the floral organ number increase (i.e. twin-flower phenotype) was significantly enhanced in the *dp1–2 sdp1* double mutant. Like *dp1–2*, flowers of the *dp1–2 sdp1* double mutant were palea-less and failed to develop the central region of palea with only palea margin pairs retained (Fig. 4F), which is different from the small palea phenotype observed in *sdp1*. Notably, most *dp1–2 sdp1* double mutant flowers (64%) exhibited increased floral organ number. Such twin-flowers were almost identical to those observed in the *dp1–2* single mutant (Figs. 4G, H), although the frequency was ~20 times higher. In addition to increased inner organ numbers found in the twin-flowers, we observed more severely fused or undifferentiated carpels and stigmas in <1% spikelets, in which degenerated ovule or undifferentiated cell mass could form (Figs. 4I, J).

### *DP1 affects the expression of E function genes and AP1 sub-family gene OsMADS15*

Since *DP1* affects floral organ identity and development, as well as floral organ number, we were curious if it regulates the expression of genes known to affect floral development, most of which are MADS

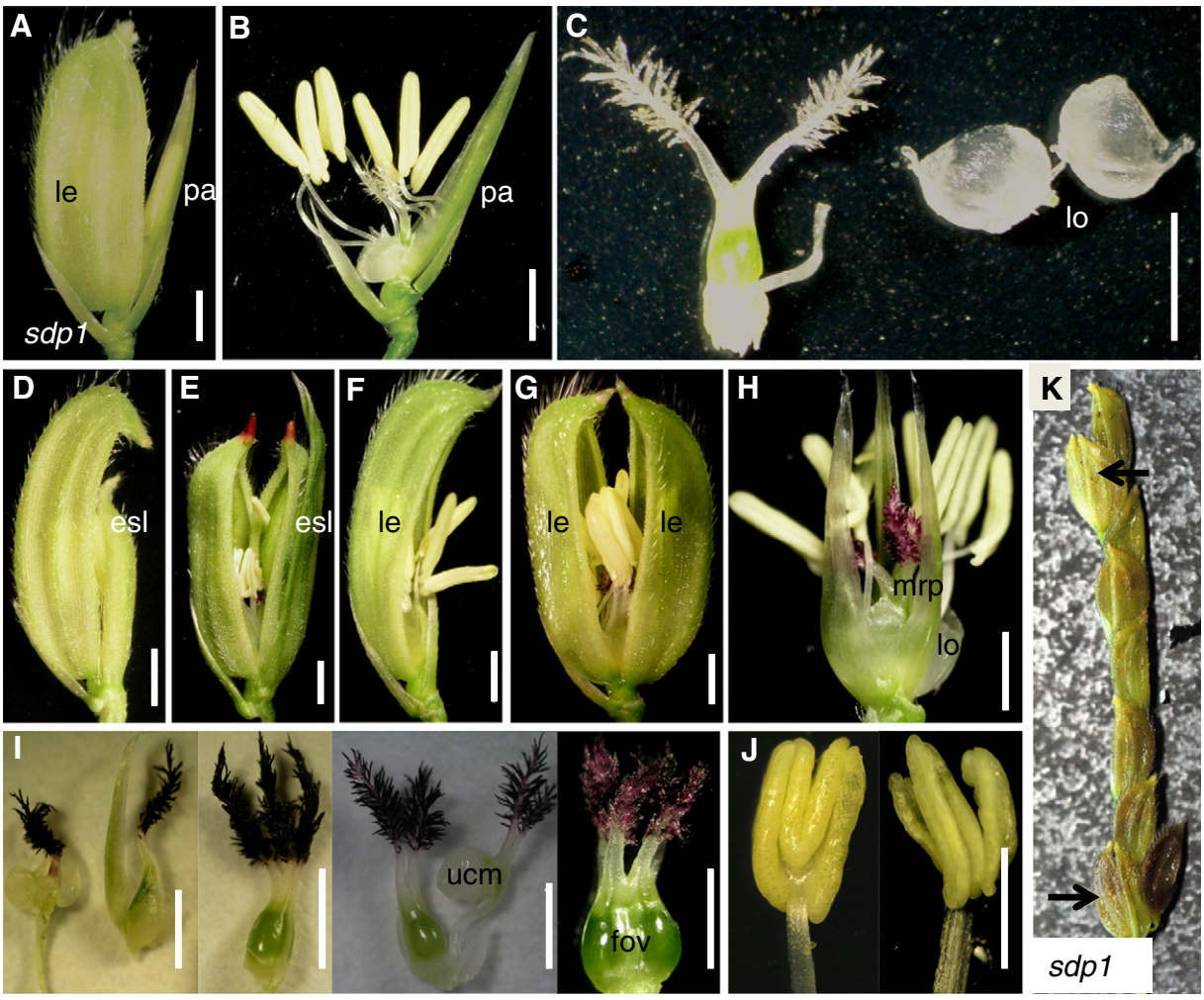


**Fig. 4.** Phenotype of *sdp1* and double mutant *dp1–2 sdp1*. (A–C) *sdp1* has a phenotype with small palea (A) but normal inner organs including stamens (B), carpel and lodicules (C). (D–J) *dp1–2 sdp1/rep1–3* phenotypes. (D) A single palealess flower with elongated sterile lemma on the palea side. (E) A twin-flower with elongated sterile lemma on the palea side. (F) A single palea-less flower. (G) A twin-flower. (H) The near-doubled inner organs of the twin-flower. (I) Variable carpel phenotypes. From leaf to right, a degenerated ovule, stigmas grew on a bract, three stigmas grew on one ovule, two stigmas grew on a filament which had undifferentiated cell mass (ucm) and four stigmas grew on one malformed ovule which was formed by two fused ovules (fov). (J) Malformed anther phenotype. Left, one filament with two fused anthers; Right, one filament with three anthers. (K) *sdp1* spikelets. Arrows indicate twin-flowers. le, lemma; pa, palea; esl, elongated sterile lemma; lo, lodicules; mrp, marginal region of palea; ucm, undifferentiated cell mess; fov, fused ovary. Sale bars = 1 mm.

family transcription factors. To this end, we performed qRT-PCR to quantify the expression of over a dozen genes in the wild type and the *dp1–2* mutant young inflorescences less than 1 cm, between 1 cm and 2 cm, and between 2 cm and 3 cm in length, in which floral organs start to initiate. We studied putative B function genes (*OsMADS2*, *OsMADS4* and *OsMADS16*), C function genes (*OsMADS3*, *OsMADS58* and *DL*), D function gene (*OsMADS13*), E function genes (*OsMADS1*, *OsMADS6*, *OsMADS7*, *OsMADS8* and *OsMADS17*), AP1/SQUA sub-family genes (*OsMADS14*, *OsMADS15* and *OsMADS18*), and *CLV1*-homolog *FON1* (Agrawal et al., 2005; Dreni et al., 2007; Kater et al., 2006; Kyozuka et al., 2000; Li et al., 2010; Moon et al., 1999; Nagasawa et al., 2003; Ohmori et al., 2009; Suzaki et al., 2004; Wang et al., 2010; Yamaguchi et al., 2006). While most of these tested genes did not show conspicuous alteration in the *dp1–2* mutant ($P > 0.05$; Fig. 5A), E function genes *OsMADS1*, *OsMADS6* and *OsMADS17*, as well as *OsMADS15* were expressed at 30%–50% of wild type levels in the *dp1–2* mutant ($P < 0.05$ according to Student's *t*-test; Figs. 5B–E and S3A–D). Interestingly, the expression patterns of *OsMADS1* and *OsMADS15* detected by in situ hybridization were not altered in the *dp1–2* mutant (Fig. S3E), indicating that *DP1* gene positively enhanced *OsMADS1* and *OsMADS15* expression quantitatively but not qualitatively.

### *Map-based cloning of DP1 and SDP1 genes*

To understand its molecular functions, we isolated the *DP1* gene by map-based cloning. We developed CAPS markers to map *DP1* to a 10 kb region (Fig. 6A). Only one predicted coding sequence, *Os06g0136900*, was annotated in the region according to the rice genome database (http://rapdb.dna.affrc.go.jp/). Sequence analysis identified a 6 bp deletion (366 nt to 371 nt) in *dp1–1*, two substitutions (A62S and H288P), a 3 bp deletion (952 nt to 954 nt), and a 6 bp insertion of two His after 39 nt in *dp1–2*, and a 51 bp deletion (396 nt to 446 nt) in *dp1-3* in the coding region (Fig. 6B). In addition, we found several polymorphism sites in the promoter region of *dp1–2* (Table S1). We introduced the *Os06g0136900* genomic fragment with its 5728 bp 5′ upstream region and 2577 bp 3′ downstream region into *dp1–2*, and found that the spikelets and floral organs were completely rescued to the wild type shape in all ten independent transgenic lines we obtained (Fig. 6C), indicating that *Os06g0136900* is the *DP1* gene.

The identity of the *DP1* gene was also confirmed by silencing *DP1* products using RNA interference. Six independent transgenic lines transformed with an inverted repeat containing a *DP1* region were generated and named *DP1i*. All transgenic plants had similar phenotypes to

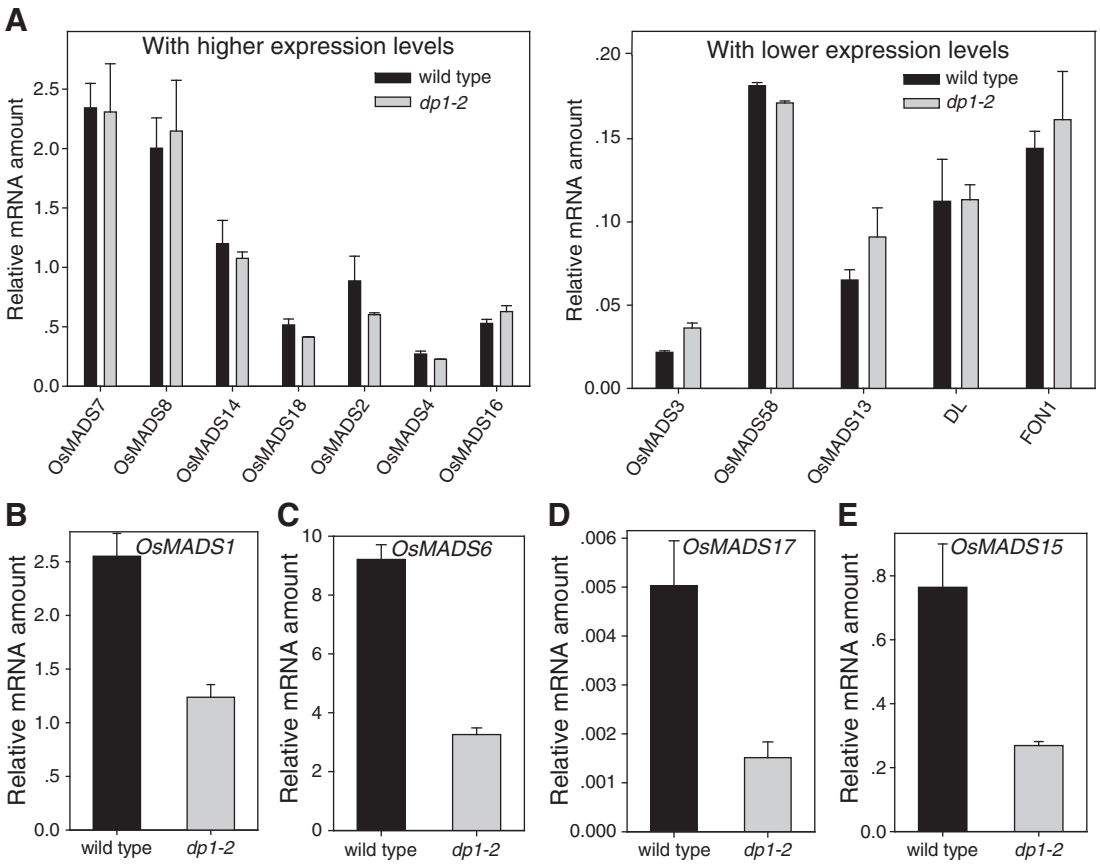


**Fig. 5.** Expression level analysis of flower development related genes. The results using 0–1 cm inflorescences were shown. (A) Expression level comparison of flower development related genes (shown as two panels classified by expression levels) between wild type and *dp1–2* ($P>0.05$ for all genes). (B–E) Comparison of *OsMADS1* (B, $P<0.001$), *OsMADS6* (C, $P<0.001$), *OsMADS17* (D, $P<0.05$) and *OsMADS15* (E, $P<0.05$) expression levels between wild type and *dp1–2*. Student's *t*-test was used to determine significant changes in expression.

*dp1* mutants (Fig. 6E). Generally, flowers of *DP1i* looked all abnormal from the overall view of the panicles (Fig. 6Ea). Several lines showed no palea but two palea margins (Fig. 3Eb, e), and others had degenerative palea (Fig. 3Ec, f). A significant number (>15%; Table 1) of flowers presented as twin-flowers, which had four palea margins and increased number of stamens and carpels (Fig. 6Ed, g). In addition, the phenotypic severities were well correlated with the *DP1* expression levels in these *DP1i* lines (Table 1; Figs. 6E, F). Notably, twin-flowers with increased floral organ number occurred more frequently in *DP1i* lines than in any *dp1* mutant, accounting for 48% in the strong line *DP1i-2* and 16.8% in the weak line *DP1i-1* (Table 1). Again, this independent experiment confirmed the identity of the *DP1* gene.

In addition, we overexpressed *DP1* in rice and obtained five transgenic lines. In tissue culture conditions, all *DP1*-overexpressing lines were severe dwarfism with rolling leaves at seedling stages (Fig. S4). We were unable to study the effects of *DP1* overexpression on floral organ development because all these *DP1*-overexpressing lines died before floral transition.

We tested the transcript levels of *DP1* in *dp1* mutants and wild type spikelets by qRT-PCR. We found that the gene expression level significantly reduced in *dp1–2* but not obviously changed in *dp1–1* or *dp1–3* (Figs. 6D and S5A, B). Thus, the decreased expression in *dp1–2* might be attributed to the DNA sequence changes in the promoter region. On the other hand, the different severity of *dp1–1* and *dp1–3* phenotypes should be only caused by their respective defects in the DP1 protein, i.e. missing 17 aa and 2 aa respectively (Fig. 7A).

To elucidate the molecular function of *SDP1*, we again isolated the gene using a map-based cloning strategy. Using a $F_2$ population of *sdp1*×cv. Minghui 63 (*Oryza sativa* spp. *indica*), *SDP1* was in a 92 kb region of chromosome 9, containing 11 annotated genes. By sequencing each gene of this region in *sdp1*, we identified a 13 nt deletion correspond to positions 111 to 123 of the annotated open reading frame in *Os09g24480* (Fig. S6). This gene was later reported as *RETARDED PALEA1* (*REP1*) (Yuan et al., 2009). We further carried out allele test and confirmed that *sdp1* is allelic to *rep1–1*, and renamed *sdp1* as *rep1–3*.

### *DP1 encodes an AT-hook protein*

*DP1* has no intron, and its full-length cDNA sequence reported by KOME database (http://cdna01.dna.affrc.go.jp/cDNA/) encodes a putative protein of 328 amino acids with a 75 bp 5′-UTR (Untranslated Region) and 214 bp 3′-UTR. The DP1 protein is a putative DNA binding protein comprising a consensus AT-hook motif, RPRGRP, and a domain of unknown function, DUF296 (Fig. 7A). A database search resulted in the identification of 45 AT-hook genes in rice (http://rapdb.dna.affrc.go.jp/) and 31 in *Arabidopsis* (http://www.arabidopsis.org/). Among them, 22 rice and 21 *Arabidopsis* AT-hook genes encode proteins also containing the DUF296 domain (Fig. S7A). Phylogenetic analysis identified one clade including DP1 and three other rice proteins and two *Arabidopsis* proteins (Fig. S7A). Sequence alignment of these six proteins indicated that they shared high homology mainly within the AT-hook motif and the DUF296 domain (Fig. 7A). The 2 aa deletion of the weak allele *dp1–1* was located between the AT-hook motif and the DUF296 domain, whereas the 17 aa deletion of the strongest allele *dp1–3* covered 12 aa of the DUF296 domain, indicating that DUF296 has an important function for DP1 (Fig. 7A). Other grasses also contain genes with both the AT-hook motif and the DUF296 domain (Fig. S7B). Notably, DP1 is closely related to the recently reported BARREN STALK FASTIGIATE1 (BAF1 (Gallavotti et al., 2011).

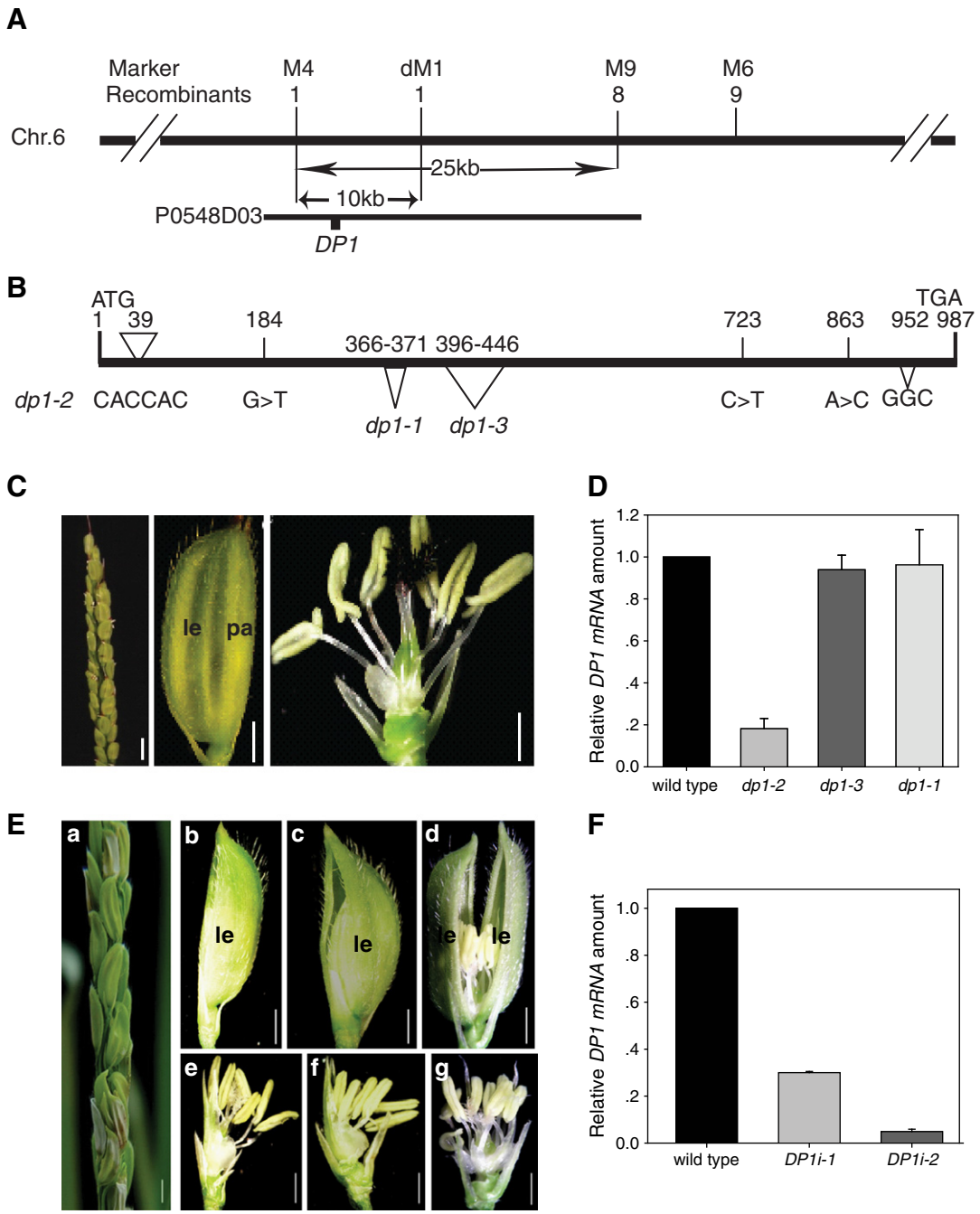


**Fig. 6.** Cloning of *DP1* and transgenic verification. (A) A schematic diagram of map-based cloning result. Distribution of the markers and their recombinants was shown. (B) A schematic diagram of the mutations sites of *dp1* alleles in *DP1* coding sequence. The triangles up and below the thick line indicate insertion and deletions respectively. (C) Spikelet phenotype of *dp1–2* plants containing a *DP1* genomic region (*DP1c*). *DP1c* has normal spikelet (left two panels) including inner organs (right panel). (D) *DP1* expression levels in three *dp1* alleles and the wild type. Inflorescences less than 1 cm were used. The expression of wild type was set at 1.0. (E) Spikelet phenotype of wild type plants containing an RNA interference construct (*DP1i*). (a) *DP1i* panicles. (b–d) *DP1i* flowers representing different levels of phenotypical changes. (e–g) Lemmas were removed to show inner organs of (b–d), respectively. Bar = 1 mm. (F) Expression analysis of *DP1* in two *DP1i* lines and the wild type. The expression level of wild type was set at 1.0.

*Nuclear localization and DNA-binding activity of DP1*

Many AT-hook proteins have been shown to activate or repress transcription of many genes by binding to AT-rich DNA sequences and modifying chromatin architecture (Aravind and Landsman, 1998; Nagano et al., 2001). To examine if DP1 as a potential DNA-binding protein is localized in the nucleus, a DP1-GFP fusion protein was transiently expressed in tobacco leaf epidermis. As expected, we found that DP1-GFP was predominantly localized to the nucleus as confirmed by DAPI staining (Fig. 7B). This subcellular localization result was further confirmed in transgenic rice plants overexpressing the DP1-GFP fusion protein (Fig. 7B). We then conducted an electrophoretic mobility shift assay using recombinant DP1 protein (DP1-MBP) to test whether the DP1 protein can bind to an AT-rich sequence (Fig. 7C). The experiment showed that DP1 was able to bind to AT probes, which were AT-rich DNA fragments, and this binding was competed by unlabeled AT probes

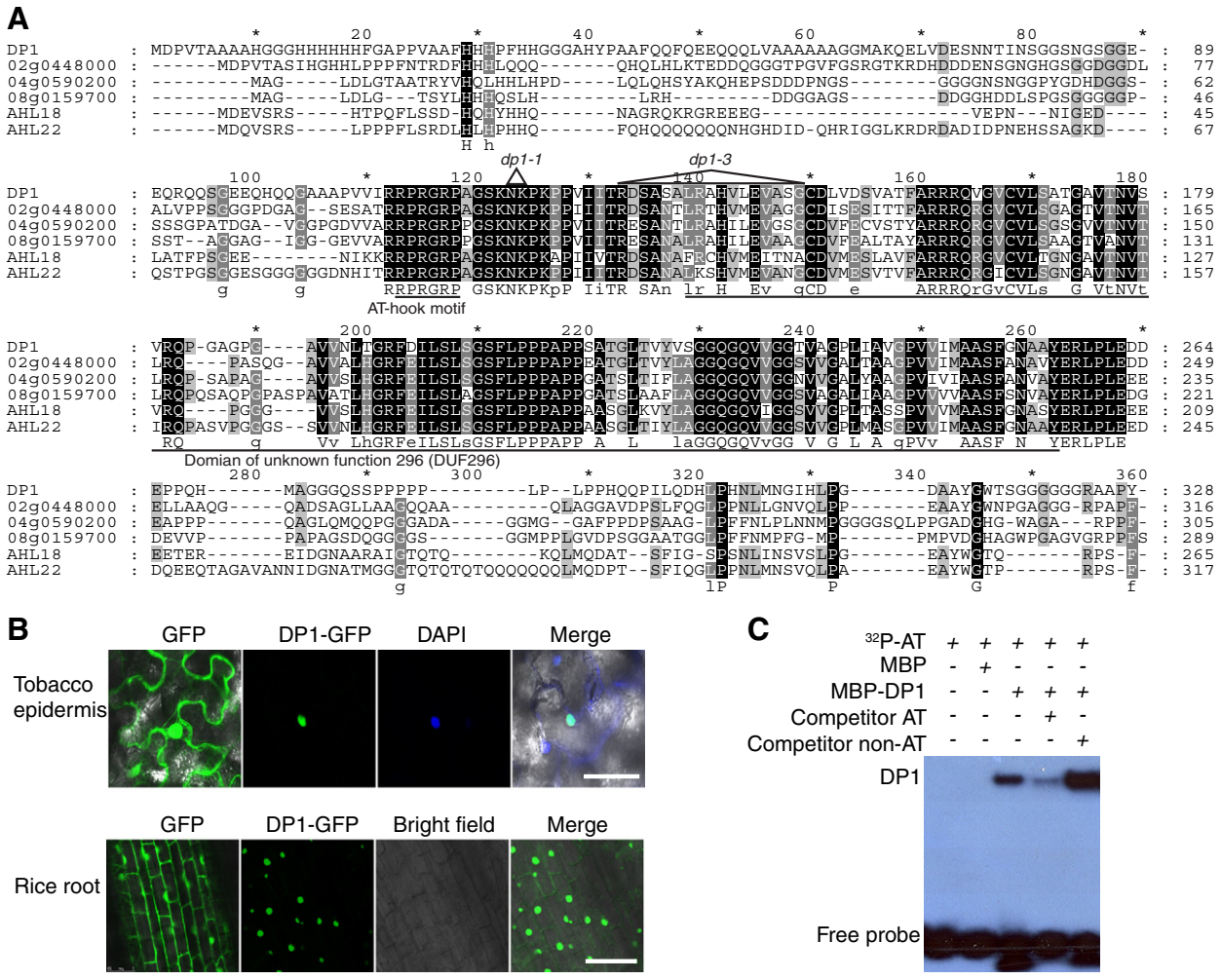


**Fig. 7.** *DP1* encodes a nuclear-localized AT-hook DNA binding protein. (A) Alignment of the closest proteins of DP1, including three rice proteins (named by their locus IDs) and two Arabidopsis proteins. AT-hook motif and the DNA-binding domain DUF296 were indicated below the sequences. The deletions of 2 aa in *dp1–1* and 17 aa in *dp1–3* are marked above the sequence. (B) DP1-GFP is located to nucleus in both tobacco epidermis and rice root. Scale bar = 50 μm. (C) DP1 can bind to AT-rich sequence. Probe AT sequence: AACACATATTTT-GATAAATTTATTACTAAA; Probe non-AT sequence: AACACACGCTTCGACGTTCCCAGGACGAAC. 50-fold excessive unlabeled probes were used as competitors.

but not by the non-AT probes with low AT content (Fig. 7C). These results suggested that DP1 is a nuclear localized AT-rich DNA binding protein.

### *Temporal and spatial expression patterns of DP1*

To gain more insight into the function of *DP1*, we examined the expression patterns of *DP1* using several approaches. First, qRT-PCR revealed that *DP1* was expressed universally in various tissues, including leaf, root, culm and inflorescence (Fig. S5C). To more precisely study the expression of *DP1*, a construct containing the *DP1* 5′ region of approximately 2 kb fused to the *GUS* reporter gene, pDP1::*GUS* was introduced into wild type rice. In eight independent lines of transgenic rice plants with pDP1::*GUS*, GUS staining confirmed the qRT-PCR result that *DP1* is expressed universally in leaf, root, culm and spikelet (Fig. S5D).

RNA in situ hybridization was further conducted to determine the temporal and spatial expression patterns of *DP1* during the flower development process. *DP1* expression was initially detected at the adaxial side of initiating panicle branch meristems, i.e. boundaries between a newly initiated panicle branch meristem and the shoot apical meristem (Figs. 8A, B). *DP1* transcripts then appeared in the entire floral meristem when the sterile lemmas initiated (Fig. 8C). After the floral meristem began to differentiate, *DP1* expression was specifically observed in the palea primordia (Figs. 8D, E) and in developing palea (Fig. 8F). Finally, after floral organ differentiation, the signals were diffused to inner organs (Fig. 8G). We could barely detect *DP1* expression in *dp1–2* inflorescences or spikelets (Figs. 8H–K), which is consistent with the very low *DP1* expression found by qRT-PCR (Figs. 6E and S5A, B).

### *DP1 is an upstream regulator of REP1/SDP1 expression*

In order to discover the relationship between *DP1* and *REP1/SDP1*, we investigated the *DP1* expression in young inflorescences (less than 1 cm) of *sdp1/rep1–3*, and *REP1/SDP1* expression in young inflorescences of *dp1–2* by qRT-PCR. While *DP1* expression level showed inconspicuous change in *sdp1/rep1–3* when compared to a wild type rice (Fig. 8M), the expression of *REP1/SDP1* was significantly decreased in *dp1–2* to about 20% that of wild type rice (Fig. 8L). Considering that even the knock-out allele of *rep1* has a much mild retarded palea development phenotype comparing with *dp1–2* (Yuan et al., 2009), it is likely that *DP1* acts upstream of *REP1/SDP1* to regulate palea development.

## Discussion

Flower development as a model for developmental biology has been extensively studied and the widely accepted ABC model successfully explained the formation of four floral whorls in a typical flower. Grasses, however, have highly specialized flowers and inflorescence structures, making it difficult to interpret the floral development process using

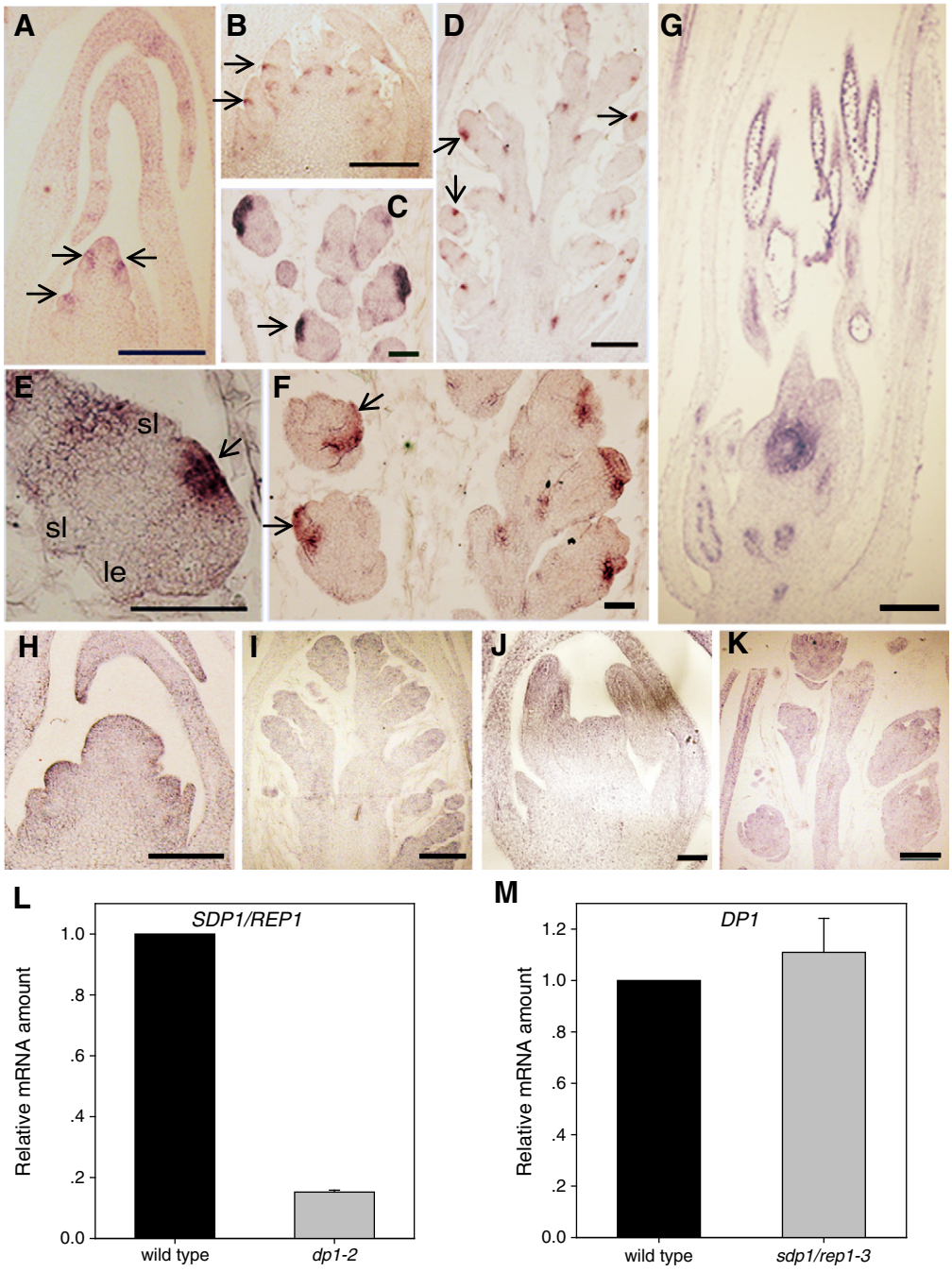


**Fig. 8.** Expression pattern of *DP1* in flower development process. (A–G) *DP1* expression in wild type. (A, B) At the stage of first (A) and secondary (B) rachis branch primodia formation. (C) At the stage after sterile lemmas initiation. (D–F) After the outer whorl organs primordium initiation (sl, sterile lemma; le, lemma). (G) At stage of floral organ differentiation. Arrows indicate specific signals. Except in (E) scale bar = 50 μm, in others, scale bars = 100 μm. (H–K) *DP1* expression in *dp1–2*. No obvious hybridization signal was detected at different stages. Scale bars = 100 μm in (H), = 200 μm in (I, J), and = 1 mm in (K). (L) *SDP1/REP1* has decreased expression level in *dp1–2* compared to wild type. (M) Comparison of *DP1* expression level between wild type and *sdp1/rep1–3*. The expression level of wild type in (L), (M) was set at 1.0.

knowledge from other model species. In this study, we identified two genes involved in rice palea and sterile lemma development, as well as the floral organ number determinacy. We further found that one of them, *DP1* controls the expression of *SDP1/REP1*, the other gene we cloned, as well as *OsMADS1*, *OsMADS6*, *OsMADS17*, and *OsMADS15* to exert its function.

### *Genetic control of palea formation*

In this study, we studied the formation of palea, a grass-specific outer whorl organ, by identifying two rice palea-defective mutants. These two mutants specifically affect palea development, but not lemma development, implied the existence of different genetics pathways controlling these two floral organs potentially in the same whorl (Figs. 1, 4). Consistent with this idea, mutations of the AP1-like *OsMADS15* gene affects palea but not lemma, in addition to other development process (Wang et al., 2010). Beside this palea specific pathway, there appears to be another pathway affecting both palea and lemma. It is not surprising that this pathway includes the SEP-like *OsMADS1* (Jeon et al., 2000; Prasad et al., 2001, 2005). More recently, two other transcription factors, *DEGENRATED HULL1* (*DH1*), a LOB family transcription factor gene, and *OsSPL16* were found affecting both palea formation and

lemma formation (Li et al., 2008; Wang et al., 2011), although their target genes remain to be identified. It is therefore likely that the formation of palea requires both an E-function like pathway including *OsMADS1*, and possibly *DH1* and *OsSPL16*, as well as a palea specific pathway containing *DP1*, *SDP1/REP1* and *OsMADS15*. It should be pointed out that this E-function may play a more important role in the outer whorls as both palea and lemma are affected more by the mutation of these genes. In fact, a novel grass-specific E-function has recently been identified, which is exerted by AGL6-like MADS box genes (Li et al., 2010; Ohmori et al., 2009; Reinheimer and Kellogg, 2009), which bias more on the development of inner whorls.

Notably, all three genes specifically affecting palea formation, *DP1*, *SDP1/REP1* and *OsMADS15*, affect only the central region of palea but not the marginal region of palea (Figs. 1–3) (Wang et al., 2010; Yuan et al., 2009). These results imply that these two parts of a palea are controlled by different genetic pathways, and that *DP1*, *SDP1/REP1* and *OsMADS15* specifically regulate the development of the central region of palea. Consistent with this idea that a palea is a fused organ with different origins, it was recently reported that flowers specifically lose the marginal region of palea but retain the central region of palea in *OsMADS6* defective mutants (Ohmori et al., 2009).

Grass leaf has similar separate origins for the marginal region and the central region. At least a double mutant of the maize narrow sheath (ns1 and ns2) genes has specific defects in the leaf margin region development, which was caused by a failure of establishing the leaf margin identity in corresponding meristematic domains (Nardmann et al., 2004; Scanlon and Freeling, 1997; Scanlon et al., 1996). It is likely that the marginal region and the central region of a grass organ originate from different meristematic domains established early during organ initiation.

In addition to affecting palea development, we found that both *DP1* and *SDP1/REP1* affected the identity of sterile lemma specifically on the palea side, especially when both genes were mutated (Figs. 1, 2, 4). Considering that rice flower, and other grass flower as well, shows zygomorphic symmetry, especially in the outer whorls (Yuan et al., 2009), both *DP1* and *SDP1/REP1* are likely downstream such signals that they only affect one side of the zygomorphic symmetric floral architecture of rice. A functionally related gene, *OsMADS15*, also affects floral development asymmetrically, although its mutation does not affect sterile lemma identity (Wang et al., 2010).

### *A possible effect of chromatin architecture modification on flower development*

In this study, we identified the causal gene for *dp1* mutants encoding an AT-hook and DUF296 containing protein (Fig. 6). We further demonstrated that DP1 is nuclear localized and can specifically bind to an AT-rich DNA fragment (Fig. 7). Such AT-hook domain containing proteins are known to co-regulate gene transcription through modification of chromatin architecture (Lim et al., 2007; Thanos and Maniatis, 1992). It is therefore likely that DP1 also control chromatin architecture to co-regulation the expression of a number of genes. Indeed, we found that *SDP1/REP1*, *OsMADS15* and *OsMADS1* genes were all suppressed in *dp1* mutants (Fig. 5), suggesting that DP1 promotes the expression of these genes. It remains unclear whether these transcriptional activations are direct or indirect.

Several related plant DUF296 domain-containing AT-hook proteins have been reported (Fig. S7), and they regulate different physiological processes including flowering, photomorphogenesis and leaf senescence (Lim et al., 2007; Street et al., 2008; Weigel et al., 2000). *DP1* appears to be the first AT-hook and DUP296 containing protein functioning in flower development. An extensively studied *Arabidopsis* AT-hook protein, SPLAYED (SYD), was found a chromatin remodeler that regulates the expression of a large number of genes, to exert its function in floral transition, stem cell maintenance, and stress signaling pathways (Kwon et al., 2005; Su et al., 2006; Wagner and Meyerowitz, 2002; Walley et al., 2008). Different from DP1 with one AT-hook motif and a conserved DUF296, SYD contains a conserved ATPase domain and two AT-hook motifs in its N-terminal region, making SYD only distantly related to DP1. More recently, a maize AT-hook protein BAF1 was reported, which is required for maize ear formation, axillary meristem initiation, and boundary region demarcation (Gallavotti et al., 2011). Similar to DP1, BAF1 contains one AT-hook motif and a DUF296 domain, which was also named the PPC domain. Our phylogenetic analysis revealed that BAF1 and DP1 are closely related and are likely orthologs (Fig. S7B). Consistently, both DP1 and BAF1 function in flower development, although specified to the formation of different organs in rice and in maize.

### *Effects of DP1 and SDP1/REP1 on floral meristem activity*

We found that the increased floral organ number phenotype of *dp1 sdp1/rep1* double mutant was very similar to those of *fon1* and *fon2/fon4* mutants (Fig. 4), indicating that the floral meristem is likely affected. Also single mutants of either gene showed this “twin-flower” phenotype at low penetration (Table 1), the combination of both mutations significantly enhanced the phenotype. In *fon1* and *fon2/fon4* mutants, the floral meristem size are enlarged, which causes the increased floral organ number (Chu et al., 2006; Suzaki et al., 2004, 2006). Consistently, we found the floral meristem in twin-flowers of *dp1-2* enlarged (Fig. S2). *FON1* and *FON2/FON4* encode homologs of *Arabidopsis* CLV1 and CLV3 respectively. It is reasonable to speculate that *DP1* and *SDP1/REP1* interplay with the WUS-CLV loop to control meristem activity. It remains to be elucidated whether the expression of *FON1* and *FON2/FON4* genes are suppressed by *DP1* and *SDP1/REP1*, or *OsWUS* expression is enhanced by *DP1* and *SDP1/REP1*, or *DP1* and *SDP1/REP1* affects both parts simultaneously. Considering that several E function genes are down-regulated in *dp1* mutants, it is possible that the reduced E function is responsible, or at least related, to the enlarged floral meristem seen in *dp1* and *dp1 sdp1/rep1* rice.

## Acknowledgments

We thank Drs. Zheng Meng and Feng Wu (Institute of Botany, CAS) for assistance with RNA in situ hybridization, Dr. Dabing Zhang (Shanghai Jiao Tong University) for providing *rep1–1* seeds. The work was supported by grants from the State Key Laboratory of Plant Genomics and the Plant Gene Research Center (Beijing) at IGDB, CAS, the National Natural Science Foundation of China (NSFC) to LH Zhu (30550005) and Q Luo (30370797 and 30760100), and the Natural Science Foundation of Yunnan Province to Q Luo (2007C0063M).

## Appendix A. Supplementary data

Supplementary data to this article can be found online at doi:10.1016/j.ydbio.2011.08.023.

## References

Agrawal, G.K., Abe, K., Yamazaki, M., Miyao, A., Hirochika, H., 2005. Conservation of the E-function for floral organ identity in rice revealed by the analysis of tissue culture-induced loss-of-function mutants of the *OsMADS1* gene. Plant Mol. Biol. 59, 125–135.

Ambrose, B.A., Lerner, D.R., Ciceri, P., Padilla, C.M., Yanofsky, M.F., Schmidt, R.J., 2000. Molecular and genetic analyses of the *Silky1* gene reveal conservation in floral organ specification between eudicots and monocots. Mol. Cell 5, 569–579.

Aravind, L., Landsman, D., 1998. AT-hook motifs identified in a wide variety of DNA binding proteins. Nucleic Acids Res. 26, 4413–4421.

Bell, A.D., Bryan, A., 1991. Plant Form: An Illustrated Guide to Flowering Plant Morphology. Oxford University Press, Oxford, New York.

Bell, A.D., Bryan, A., 2008. Plant Form: An Illustrated Guide to Flowering Plant Morphology. Timber Press, Portland, OR.

Bommert, P., Satoh-Nagasawa, N., Jackson, D., Hirano, H.Y., 2005. Genetics and evolution of inflorescence and flower development in grasses. Plant Cell Physiol. 46, 69–78.

Bowman, J.L., Smyth, D.R., Meyerowitz, E.M., 1991. Genetic interactions among floral homeotic genes of Arabidopsis. Development 112, 1–20.

Chu, H., Qian, Q., Liang, W., Yin, C., Tan, H., Yao, X., Yuan, Z., Yang, J., Huang, H., Luo, D., Ma, H., Zhang, D., 2006. The *FLORAL ORGAN NUMBER4* gene encoding a putative ortholog of Arabidopsis CLAVATA3 regulates apical meristem size in rice. Plant Physiol. 142, 1039–1052.

Clifford, H.T. (Ed.), 1987. Spikelet and Floral Morphology. Smithsonian Institution Press, Washington, DC.

Coen, E.S., Meyerowitz, E.M., 1991. The war of the whorls: genetic interactions controlling flower development. Nature 353, 31–37.

Dreni, L., Jacchia, S., Fornara, F., Fornari, M., Ouwerkerk, P.B.F., An, G.H., Colombo, L., Kater, M.M., 2007. The D-lineage MADS-box gene OsMADS13 controls ovule identity in rice. Plant J. 52, 690–699.

Gallavotti, A., Malcomber, S., Gaines, C., Stanfield, S., Whipple, C., Kellogg, E., Schmidt, R.J., 2011. BARREN STALK FASTIGIATE1 is an AT-hook protein required for the formation of maize ears. Plant Cell 23, 1756–1771.

Hiei, Y., Ohta, S., Komari, T., Kumashiro, T., 1994. Efficient transformation of rice (*Oryza Sativa* L) mediated by *Agrobacterium* and sequence-analysis of the boundaries of the T-DNA. Plant J. 6, 271–282.

Ikeda, K., Sunohara, H., Nagato, Y., 2004. Developmental course of inflorescence and spikelet in rice. Breed. Sci. 54, 147–156.

Iwata, N., Satoh, H., Omura, T., 1984. The relationships between chromosomes identified cytologically and linkage groups. Rice Genet. Newsl. 1, 128–132.

Jefferson, R.A., 1989. The GUS reporter gene system. Nature 342, 837–838.

Jeon, J.S., Jang, S., Lee, S., Nam, J., Kim, C., Lee, S.H., Chung, Y.Y., Kim, S.R., Lee, Y.H., Cho, Y.G., An, G., 2000. *leafy hull sterile1* is a homeotic mutation in a rice MADS box gene affecting rice flower development. Plant Cell 12, 871–884.

Kang, H.G., Jeon, J.S., Lee, S., An, G., 1998. Identification of class B and class C floral organ identity genes from rice plants. Plant Mol. Biol. 38, 1021–1029.

Kater, M.M., Dreni, L., Colombo, L., 2006. Functional conservation of MADS-box factors controlling floral organ identity in rice and *Arabidopsis*. J. Exp. Bot. 57, 3433–3444.

Kellogg, E.A., 2001. Evolutionary history of the grasses. Plant Physiol. 125, 1198–1205.

Krizek, B.A., Fletcher, J.C., 2005. Molecular mechanisms of flower development: an armchair guide. Nat. Rev. Genet. 6, 688–698.

Kwon, C.S., Chen, C., Wagner, D., 2005. WUSCHEL is a primary target for transcriptional regulation by SPLAYED in dynamic control of stem cell fate in Arabidopsis. Genes Dev. 19, 992–1003.

Kyozuka, J., Kobayashi, T., Morita, M., Shimamoto, K., 2000. Spatially and temporally regulated expression of rice MADS box genes with similarity to Arabidopsis class A, B and C genes. Plant Cell Physiol. 41, 710–718.

Li, G.S., Meng, Z., Kong, H.Z., Chen, Z.D., Theissen, G., Lu, A.M., 2005. Characterization of candidate class A, B and E floral homeotic genes from the perianthless basal angiosperm *Chloranthus spicatus* (Chloranthaceae). Dev. Genes Evol. 215, 437–449.

Li, A., Zhang, Y., Wu, X., Tang, W., Wu, R., Dai, Z., Liu, G., Zhang, H., Wu, C., Chen, G., Pan, X., 2008. DH1, a LOB domain-like protein required for glume formation in rice. Plant Mol. Biol. 66, 491–502.

Li, H., Liang, W., Jia, R., Yin, C., Zong, J., Kong, H., Zhang, D., 2010. The AGL6-like gene OsMADS6 regulates floral organ and meristem identities in rice. Cell Res. 20, 299–313.

Lim, P.O., Kim, Y., Breeze, E., Koo, J.C., Woo, H.R., Ryu, J.S., Park, D.H., Beynon, J., Tabrett, A., Buchanan-Wollaston, V., Nam, H.G., 2007. Overexpression of a chromatin architecture-controlling AT-hook protein extends leaf longevity and increases the post-harvest storage life of plants. Plant J. 52, 1140–1153.

Luo, Q., Zhou, K., Zhao, X., Zeng, Q., Xia, H., Zhai, W., Xu, J., Wu, X., Yang, H., Zhu, L., 2005. Identification and fine mapping of a mutant gene for palealess spikelet in rice. Planta 221, 222–230.

Matsushita, A., Furumoto, T., Ishida, S., Takahashi, Y., 2007. AGF1, an AT-hook protein, is necessary for the negative feedback of AtGA3ox1 encoding GA 3-oxidase. Plant Physiol. 143, 1152–1162.

Moon, Y.H., Kang, H.G., Jung, J.Y., Jeon, J.S., Sung, S.K., An, G., 1999. Determination of the motif responsible for interaction between the rice APETALA1/AGAMOUS-LIKE9 family proteins using a yeast two-hybrid system. Plant Physiol. 120, 1193–1203.

Nagano, Y., Furuhashi, H., Inaba, T., Sasaki, Y., 2001. A novel class of plant-specific zinc-dependent DNA-binding protein that binds to A/T-rich DNA sequences. Nucleic Acids Res. 29, 4097–4105.

Nagasawa, N., Miyoshi, M., Sano, Y., Satoh, H., Hirano, H., Sakai, H., Nagato, Y., 2003. *SUPERWOMAN1* and *DROOPING LEAF* genes control floral organ identity in rice. Development 130, 705–718.

Nardmann, J., Ji, J., Werr, W., Scanlon, M.J., 2004. The maize duplicate genes narrow sheath1 and narrow sheath2 encode a conserved homeobox gene function in a lateral domain of shoot apical meristems. Development 131, 2827–2839.

Nieto-Sotelo, J., Ichida, A., Quail, P.H., 1994. PF1: an A-T hook-containing DNA binding protein from rice that interacts with a functionally defined d(AT)-rich element in the oat phytochrome A3 gene promoter. Plant Cell 6, 287–301.

Niwa, Y., Hirano, T., Yoshimoto, K., Shimizu, M., Kobayashi, H., 1999. Non-invasive quantitative detection and applications of non-toxic, S65T-type green fluorescent protein in living plants. Plant J. 18, 455–463.

Ohmori, S., Kimizu, M., Sugita, M., Miyao, A., Hirochika, H., Uchida, E., Nagato, Y., Yoshida, H., 2009. *MOSAIC FLORAL ORGANS1*, an *AGL6*-like MADS box gene, regulates floral organ identity and meristem fate in rice. Plant Cell 21, 3008–3025.

Prasad, K., Vijayraghavan, U., 2003. Double-stranded RNA interference of a rice PI/GLO paralog, OsMADS2, uncovers its second-whorl-specific function in floral organ patterning. Genetics 165, 2301–2305.

Prasad, K., Sriram, P., Kumar, C.S., Kushalappa, K., Vijayraghavan, U., 2001. Ectopic expression of rice *OsMADS1* reveals a role in specifying the lemma and palea, grass floral organs analogous to sepals. Dev. Genes Evol. 211, 281–290.

Prasad, K., Parameswaran, S., Vijayraghavan, U., 2005. OsMADS1, a rice MADS-box factor, controls differentiation of specific cell types in the lemma and palea and is an early-acting regulator of inner floral organs. Plant J. 43, 915–928.

Pryor, K.D., Leiting, B., 1997. High-level expression of soluble protein in *Escherichia coli* using a His(6)-tag and maltose-binding-protein double-affinity fusion system. Protein Expr. Purif. 10, 309–319.

Qin, R.Z., Cheng, Z.J., Guo, X.P., 2005. The establishment of mutant pool using anther culture of autotetrapolyploid rice. Acta Agron. Sin. 31, 392–394.

Reinheimer, R., Kellogg, E.A., 2009. Evolution of *AGL6-like* MADS box genes in grasses (Poaceae): ovule expression is ancient and palea expression is new. Plant Cell 21, 2591–2605.

Scanlon, M.J., Freeling, M., 1997. Clonal sectors reveal that a specific meristematic domain is not utilized in the maize mutant narrow sheath. Dev. Biol. 182, 52–66.

Scanlon, M.J., Schneeberger, R.G., Freeling, M., 1996. The maize mutant narrow sheath fails to establish leaf margin identity in a meristematic domain. Development 122, 1683–1691.

Schmidt, R.J., Ambrose, B.A., 1998. The blooming of grass flower development. Curr. Opin. Plant Biol. 1, 60–67.

Shinozuka, Y., Kojima, S., Shomura, A., Ichimura, H., Yano, M., Yamamoto, K., Sasaki, T., 1999. Isolation and characterization of rice MADS box gene homologues and their RFLP mapping. DNA Res. 6, 123–129.

Sparkes, I.A., Runions, J., Kearns, A., Hawes, C., 2006. Rapid, transient expression of fluorescent fusion proteins in tobacco plants and generation of stably transformed plants. Nat. Protoc. 1, 2019–2025.

Street, I.H., Shah, P.K., Smith, A.M., Avery, N., Neff, M.M., 2008. The AT-hook-containing proteins SOB3/AHL29 and ESC/AHL27 are negative modulators of hypocotyl growth in *Arabidopsis*. Plant J. 54, 1–14.

Su, Y.H., Kwon, C.S., Bezhani, S., Huvermann, B., Chen, C.B., Peragine, A., Kennedy, J.F., Wagner, D., 2006. The N-terminal ATPase AT-hook-containing region of the Arabidopsis chromatin-remodeling protein SPLAYED is sufficient for biological activity. Plant J. 46, 685–699.

Suzaki, T., Sato, M., Ashikari, M., Miyoshi, M., Nagato, Y., Hirano, H.Y., 2004. The gene FLORAL ORGAN NUMBER1 regulates floral meristem size in rice and encodes a leucine-rich repeat receptor kinase orthologous to Arabidopsis CLAVATA1. Development 131, 5649–5657.

Suzaki, T., Toriba, T., Fujimoto, M., Tsutsumi, N., Kitano, H., Hirano, H.Y., 2006. Conservation and diversification of meristem maintenance mechanism in *Oryza sativa*: function of the *FLORAL ORGAN NUMBER2* gene. Plant Cell Physiol. 47, 1591–1602.

Thanos, D., Maniatis, T., 1992. The high mobility group protein HMG I(Y) is required for NF-kappa B-dependent virus induction of the human IFN-beta gene. Cell 71, 777–789.

Thompson, B.E., Bartling, L., Whipple, C., Hall, D.H., Sakai, H., Schmidt, R., Hake, S., 2009. Bearded-ear encodes a MADS box transcription factor critical for maize floral development. Plant Cell 21, 2578–2590.

Wagner, D., Meyerowitz, E.M., 2002. SPLAYED, a novel SWI/SNF ATPase homolog, controls reproductive development in Arabidopsis. Curr. Biol. 12, 85–94.

Walley, J.W., Rowe, H.C., Xiao, Y., Chehab, E.W., Kliebenstein, D.J., Wagner, D., Dehesh, K., 2008. The chromatin remodeler SPLAYED regulates specific stress signaling pathways. PLoS Pathog. 4, e1000237.

Wang, K.J., Tang, D., Hong, L.L., Xu, W.Y., Huang, J., Li, M., Gu, M.H., Xue, Y.B., Cheng, Z.K., 2010. *DEP* and *AFO* regulate peproductive habit in rice. PLoS Genet. 6, e1000818.

Wang, S.-S., Wang, C.-S., Tseng, T.-H., Hou, Y.-L., Chen, K.-Y., 2011. High-resolution genetic mapping and candidate gene identification of the SLP1 locus that controls glume development in rice. Theor. Appl. Genet. 122, 1489–1496.

Weigel, D., Ahn, J.H., Blazquez, M.A., Borevitz, J.O., Christensen, S.K., Fankhauser, C., Ferrandiz, C., Kardailsky, I., Malancharuvil, E.J., Neff, M.M., Nguyen, J.T., Sato, S., Wang, Z.Y., Xia, Y.J., Dixon, R.A., Harrison, M.J., Lamb, C.J., Yanofsky, M.F., Chory, J., 2000. Activation tagging in Arabidopsis. Plant Physiol. 122, 1003–1013.

Whipple, C.J., Zanis, M.J., Kellogg, E.A., Schmidt, R.J., 2007. Conservation of B class gene expression in the second whorl of a basal grass and outgroups links the origin of lodicules and petals. Proc. Natl. Acad. Sci. U. S. A. 104, 1081–1086.

Whipple, C.J., Hall, D.H., DeBlasio, S., Taguchi-Shiobara, F., Schmidt, R.J., Jackson, D.P., 2010. A conserved mechanism of bract suppression in the grass family. Plant Cell. 22, 565–578.

Xiao, H., Wang, Y., Liu, D.F., Wang, W.M., Li, X.B., Zhao, X.F., Xu, J.C., Zhai, W.X., Zhu, L.H., 2003. Functional analysis of the rice AP3 homologue OsMADS16 by RNA interference. Plant Mol. Biol. 52, 957–966.

Xiao, C.W., Chen, F.L., Yu, X.H., Lin, C.T., Fu, Y.F., 2009. Over-expression of an AT-hook gene, AHL22, delays flowering and inhibits the elongation of the hypocotyl in Arabidopsis thaliana. Plant Mol. Biol. 71, 39–50.

Yadav, S.R., Prasad, K., Vijayraghavan, U., 2007. Divergent regulatory OsMADS2 functions control size, shape and differentiation of the highly derived rice floret second-whorl organ. Genetics 176, 283–294.

Yamaguchi, T., Hirano, H.Y., 2006. Function and diversification of MADS-box genes in rice. ScientificWorldJournal 6, 1923–1932.

Yamaguchi, T., Lee, D.Y., Miyao, A., Hirochika, H., An, G.H., Hirano, H.Y., 2006. Functional diversification of the two C-class MADS box genes OSMADS3 and OSMADS58 in Oryza sativa. Plant Cell 18, 15–28.

Yin, Y.H., Vafeados, D., Tao, Y., Yoshida, S., Asami, T., Chory, J., 2005. A new class of transcription factors mediates brassinosteroid-regulated gene expression in *Arabidopsis*. Cell 120, 249–259.

Yoshimura, A., Ideta, O., Iwata, N., 1997. Linkage map of phenotype and RFLP markers in rice. Plant Mol. Biol. 35, 49–60.

Yuan, Z., Gao, S., Xue, D.W., Luo, D., Li, L.T., Ding, S.Y., Yao, X., Wilson, Z.A., Qian, Q., Zhang, D.B., 2009. RETARDED PALEA1 controls palea development and floral zygomorphy in rice. Plant Physiol. 149, 235–244.

Zanis, M.J., 2007. Grass spikelet genetics and duplicate gene comparisons. Int. J. Plant Sci. 168, 93–110.